# Virtual drilling in 3-D objects reconstructed by shape-based interpolation

Adrian G. Borş[1], Lefteris Kechagias[2], Ioannis Pitas[2]

[1] Department of Computer Science, University of York
York YO10 5DD, U.K. - E-mail: adrian.bors@cs.york.ac.uk
[2] Department of Informatics, University of Thessaloniki, Box 451,
54006 Thessaloniki, Greece - E-mail: {lkechagi,pitas}@zeus.csd.auth.gr

**Abstract.** In this paper we propose a virtual drilling algorithm which is applied on 3-D objects. We consider that initial we are provided with a sparse set of parallel and equi-distant slices of a 3-D object. We propose a volumetric interpolation algorithm for recovering the 3-D shape from the given set of slices. This algorithm employs a morphology morphing transform. Drilling is simulated on the resulting volume as a 3-D erosion operation. The proposed technique is applied for virtual drilling of teeth considering various burr shapes as erosion elements.

## 1 Introduction

3-D object representation and processing simulation is required in many fields such as medicine, architecture, computer aided design, etc. [1–3]. Very often we are not provided with the complete information about the object to be modeled and processed. In this paper we show how virtual processing operations can be simulated on volumes described by means of a group of slices representing parallel sections of its structure. Depending on the type of the object we represent such images can be acquired by Computer Tomography (CT), Magnetic Resonance Imaging (MRI) or by mechanical slicing and digitization. Usually, the pixel size within a slice is different from the spacing between two adjacent slices. In such situations it is necessary to interpolate additional slices in order to obtain an accurate volumetric description of the object. In this paper we employ mathematical morphology for reconstructing a full 3-D shape from a group of slices and afterwards for modeling 3-D drilling in the resulting shape.

There are two main categories of interpolation techniques for reconstructing objects from sparse sets: grey-level and shape-based. Grey-level interpolation methods employ nearest-neighbor, splines, linear [2], or polynomial interpolation. Other algorithms employ feature matching [4] or homogeneity similarity [5] for determining the direction of interpolation. Interpolation of additional cross-sections from shape contours in vector form is described in [6]. A distance function from each pixel to the object boundary is considered for interpolation in [1]. Extensions of this algorithm are proposed in [7, 8]. An algorithm which uses the elastic matching interpolation, spline theory and surface consistency is

considered in [9]. In [10] each slice is eroded by a morphological operator until its number of pixels reaches the mean of those from the slices to be interpolated. A mixed shape and grey level based interpolation method is proposed in [11].

A mathematical morphology based function interpolation algorithm called the skeleton by influence zones transform (SKIZ) has been employed in [12]. The SKIZ transform interpolates by employing dilations of the intersection and of the complementary of the union of two sets [12]. However, such an approach does not correspond to a natural morphing of one set into the next one. In this paper we propose a morphing procedure for estimating the intermediary slices of the two given sets. The morphing transforms two neighboring sets by using combinations of dilations and erosions. The interpolated set corresponds to the idempotency of the two morphed sets after a certain number of iterations. This produces a new set sharing similarities in shape with both initial sets. The morphing transformation is applied repeatedly onto the new stack of interpolated sets until we recover an appropriate object shape.

After reconstructing the 3-D volumes we simulate a drilling operation. Virtual surgery using 3-D data visualization has lately attracted a lot of attention due to its potential use in surgical intervention planning and training [14]. We propose a morphological algorithm using 3-D structural elements for simulating drilling. Virtual drilling is modeled as a succession of volumetric erosions oriented along the chosen direction. The paper is organized as follows. Section 2 describes the interpolation algorithm and Section 3 the simulation of drilling using a 3-D operator. In Section 4 we provide experimental results when applying the proposed virtual drilling tool on a set of teeth reconstructed by interpolation, while the conclusions of this study are drawn in Section 5.

## 2 Geometrically constrained 3-D interpolation

Let us assume that we have two sets $X_i$ and $X_{i+1}$, which are sharing at least one common point $X_i \bigcap X_{i+1} \neq \emptyset$. We align these sets according to an $(n-1)$-dimensional hyperplane (axis for 2-D sets) using matching or a centering operation. Let us consider $X_{i,m}$ an element (pixel in 2-D or voxel in 3-D) contained into the set $X_i$, where $m$ denotes an ordering number and denote the complement (background) of the set $X_i$ by $X_i^c = E - X_i$. After alignment, each element $X_{i,m}$ in one set will have a corresponding element which may be a member of the other set $X_{i+1,m} \in X_{i+1}$, or may be part of its background $X_{i+1,m}^c \in X_{i+1}^c$.

Our morphing transformation ensures a smooth transition from one shape set to the other one by means of generating several intermediary sets. Let us consider the elements located on the boundary set, denoted by $C_i$ :

$$C_i = \{X_{i,m} \in X_i |\ \exists X_{i,l}^c\ l \in \mathcal{N}_{B_1}(X_{i,m})\} \tag{1}$$

where $\mathcal{N}_{B_1}(X_{i,m})$ denotes the neighborhood of the location $X_{i,m}$, having the same size and shape as the structuring element $B_1$. In our morphing operation, the elements of a boundary set $C_i$ are changed differently according to their correspondences from the second given set $X_{i+1}$. These changes are defined in terms

of mathematical morphology basic operations such as dilations and erosions [13]. The dilation of a set $A$ by the structuring element $B$ is given by :

$$A \oplus B = \bigcup_{b \in B} A_b \tag{2}$$

where $\oplus$ denotes dilation and $A_b$ represents a structuring element centered onto an element of the set $A$. The erosion of a set $A$ by using the structuring element $B$ is given by :

$$A \ominus B = \bigcap_{b \in B} A_b \tag{3}$$

where $\ominus$ denotes erosion. These operations correspond to the Minkowski set addition and subtraction. The most commonly used structuring element is the elementary ball of dimension $n$. The dilation with the elementary ball, *i.e.* for $n = 1$, expands the given set with a uniform layer of elements while the erosion operator takes out such a layer from the given set. The structuring element considered in this paper consists of a pixel and its horizontal and vertical immediate neighbors. We can identify three possible correspondence cases for the elements of the two aligned sets. One situation occurs when the border region of one set corresponds to the interior of the other set. In this case we dilate the border elements :

$$\begin{array}{l} \text{If} \quad X_{i,m} \in C_i \wedge X_{i+1,m} \notin C_{i+1} \\ \text{then} \quad \text{perform } X_{i,m} \oplus B_1 \end{array} \tag{4}$$

where $B_1$ is the structuring element for the set $X_i$. A second case occurs when the border region of one set corresponds to the background of the other set. In this situation we have erosions of the boundary elements :

$$\begin{array}{l} \text{If} \quad X_{i,m} \in C_i \wedge \exists\, X^c_{i+1,m} \\ \text{then} \quad \text{perform } X_{i,m} \ominus B_1 \end{array} \tag{5}$$

No modifications are performed when both corresponding elements are members of their sets boundary :

$$\begin{array}{l} \text{If} \quad X_{i,m} \in C_i \wedge X_{i+1,m} \in C_{i+1} \\ \text{then} \quad \text{perform no change} \end{array} \tag{6}$$

The last situation corresponds to the regions where the two sets coincide locally and no change is necessary, while (4) and (5) correspond to morphing transformations.

By including all these local changes we define the following morphing transformation applied on the set $X_i$ depending onto the set $X_{i+1}$ and on the structuring element $B_1$ :

$$f(X_i|X_{i+1}, B_1) = [(X_i \ominus B_1) \bigcup ((X_i \bigcap X_{i+1}) \oplus B_1)] \bigcap (X_i \bigcup X_{i+1}) \tag{7}$$

A similar morphing operation $f(X_{i+1}|X_i, B_2)$ is defined onto the set $X_{i+1}$ depending on the set $X_i$ and on the structuring element $B_2$. The proposed morphing transformation is illustrated in Figure 1.

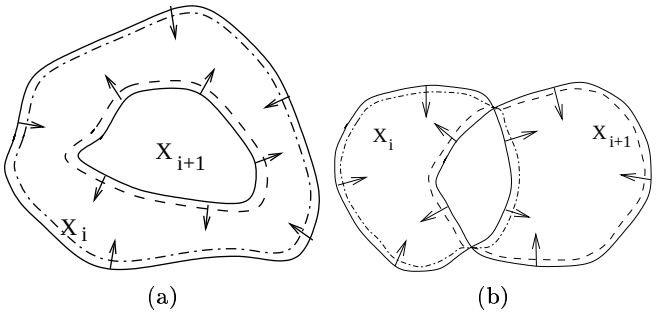


**Fig. 1.** Exemplification of mathematical morphology morphing. The result produced by equation $f(X_{i+1}|X_i, B_2)$ is represented with dashed lines while the result produced by equation $f(X_i|X_{i+1}, B_1)$ is represented with dot-dashed lines: (a) $(X_i \ominus B_1) \supset (X_{i+1} \oplus B_2)$; (b) $X_i - X_{i+1} \neq \emptyset$ and $X_{i+1} - X_i \neq \emptyset$.

The morphing operation defined by $f(X_i|X_{i+1}, B_1)$ and by $f(X_{i+1}|X_i, B_2)$ is applied iteratively onto the sets resulted from the previous morphings. For isotropic interpolation we use identical structuring elements, $B_1 = B_2 = B$, when morphing the two sets. The succession of morphing operations creates new sets starting from the two initial extremes. With each iteration these sets are closer in shape and size to each other. Eventually, the morphological transformations processing each slice will lead to the idempotency of the resulting sets. This set will represent the resulting interpolation.

This procedure can be easily extended for gray scale objects. In our approach we employ bilinear gray-level interpolation in the overlapping area of the two sets $(X_i \bigcap X_{i+1})$. In the regions where only one of the sets is defined (*i.e.* $X_i - X_{i+1} \neq \emptyset$ and $X_{i+1} - X_i \neq \emptyset$) we replicate the gray level values of the existing set for the interpolated slice.

## 3 Simulating drilling by volumetric erosion

Shape-based interpolation provides us with the 3-D object reconstruction. We need the reconstructed volume in order to simulate virtual processing operations. In the following we propose a mathematical morphology based system for simulating drilling. Let us consider that the volume is made up of isotropic material and that the effects of drilling do not depend on the direction. The drilling of the 3-D volume proceeds along a certain direction. Let us consider a parametric spherical coordinate system in which the direction is shown by two angles ($\theta$,$\phi$), where $\theta$ represents the angle made by the drilling direction with the image plane ($x$,$y$) and $\phi$ represents the angle made by the projection of the drilling direction on the image plane with the horizontal axis $x$. The drilling of a volume $\mathcal{O}$ produces a drilled volume, denoted as $\breve{\mathcal{O}}$, and can be represented as a succession of erosions with a volumetric structuring element denoted as $B^{(3)}$ :

$$\breve{\mathcal{O}} = \mathcal{O}(x, y, z) \ominus B^{(3)} \tag{8}$$

where $(x,y,z)$ denotes the point where the drilling is applied. The eroded voxels have assigned the value of the background while the object voxels corresponding to the surface of the structuring element become part of the boundary of the new object $\breve{\mathcal{O}}$. Drilling is simulated by successively eroding volumes of the 3-D structuring element size in the given direction. The drilling direction is shown by the following parametric equations :

$$x(i) = x(i-1) - d\cos(\theta)\cos(\phi) \tag{9}$$

$$y(i) = y(i-1) - d\cos(\theta)\sin(\phi) \tag{10}$$

$$z(i) = z(i-1) - d\sin(\theta) \tag{11}$$

where $d$ is the width of the drilling element in the direction of the drilling. and where the starting drilling point has the coordinates $(x(0),y(0),z(0))$. The number of times the 3-D erosion is applied depends on the speed and duration of the drilling.

We can significantly speed up the erosion process by changing the reference system from being centered on the user position into considering the processed 3-D object as the reference. In this case we replace the heavy burden of calculating the directional erosion with rotating the entire volume such that the direction of drilling becomes parallel with $z$ axis. We consider three shapes for modeling the volumetric erosion element: spherical, cylindrical and conical. At each erosion we extract a volume with the shape given by the corresponding structural element $B^{(3)}$. The corresponding region of the volume $\mathcal{O}$ has assigned the same grey level as its background, denoted as $\mathcal{O}^c$. In this case the erosion with the spherical element at the iteration $i$ is modeled by :

$$\{(x,y,z) \in \breve{\mathcal{O}},\ (x-x_{IM})^2 + (y-y_{IM})^2 + (z-z(i))^2 < d^2\} \in \breve{\mathcal{O}}^c \tag{12}$$

where $d$ is the radius of the spherical erosion element and $(x_{IM},y_{IM})$ are the coordinates of the 3-D object point projection on the image plane, where the erosion takes place. The direction of erosion is considered perpendicular onto the image plane in this case. When employing the cylindrical erosion element, the local drilling effect is given by :

$$\{(x,y,z) \in \breve{\mathcal{O}},\ z(i) > z > z(i) - d, (x-x_{IM})^2 + (y-y_{IM})^2 < R^2\} \in \breve{\mathcal{O}}^c \tag{13}$$

where $R$ is the radius and $d$ is the height of the cylindrical erosion element. The depth is conventionally considered as a negative number. For the conical erosion element, the local drilling effect is simulated by :

$$\{(x,y,z) \in \breve{\mathcal{O}},\ z(i) > z > z(i) - d, (x-x_{IM)})^2 + (y-y_{IM})^2 < \left[(z(i)-z)\frac{R}{d}\right]^2\} \in \breve{\mathcal{O}}^c \tag{14}$$

where $R$ and $d$ are the conical erosion element radius and height, respectively. In this case the drilling direction is identical with that of the projection ray used for the volumetric visualization (we have used a parallel ray tracing algorithm). The changes in the volume rendering are localized only in an area around $(x_{IM},y_{IM})$ depending on the drilling tool size. This contributes to a significant computational complexity reduction.

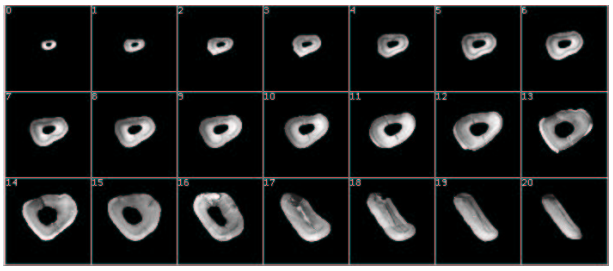

**Fig. 2.** Segmented and aligned set of slices for an incisor

## 4 Simulation results

We have applied this algorithm in virtual dentistry. We employ the interpolation algorithm to reconstruct teeth. Afterwards, we apply the virtual drilling algorithm on the reconstructed 3-D teeth. In our simulations we consider three different types of teeth: an incisor (single root), a premolar (two roots) and a molar (three roots). Teeth from each of these categories have been mechanically sliced and digitized. The teeth boundaries as well as the root canals are segmented in each slice and the resulting object slices are aligned using a semi-automatic procedure. Initial slices after alignment are displayed in Figure 2 for an incisor. We have used the morphological interpolation algorithm described in Section 2 in order to reconstruct the tooth from the given initial group of slices. Tooth cross-sections are interpolated between each two consecutive slices. In the case of the incisor, the interpolation algorithm is applied recursively four times. Thus we obtain 336 interpolated slices from 22 original slices. The 3-D reconstruction from two different viewing angles are shown in Figures 3a, 3b, for the incisor, in Figures 3c, 3d, for the premolar and in Figures 3e, 3f for the molar, respectively. This result shows a smooth transition interpolating well even between slices having large geometrical shape variations. The morphology of the reconstructed tooth is accurate despite the fact that most of the slices have been reconstructed by interpolation.

We have compared the mathematical morphology interpolation algorithm with a linear interpolation algorithm. The linear interpolation algorithm takes the midpoints of the line segments between pixels on object contours of the two slices, in both $x$ (horizontal) and $y$ (vertical) directions as the interpolated slice contour. We have applied the linear interpolation algorithm on the incisor sequence displayed in Figure 2. For assessing the performance of the interpolation algorithms we have devised the following objective measure. Let $X_i$, $X_{i+1}$ and $X_{i+2}$ be three original tooth slices and $\hat{X}_{i+1}$ be the result of interpolating $X_i$ and $X_{i+2}$. Let $|X|$ denote set cardinality. The ratio $|XOR(X_{i+1}, \hat{X}_{i+1})|/|X_{i+1}|$, representing the percentage of wrongly estimated pixels, can be used as a performance measure. In Table 1 we provide the results for reconstructing three different slices from the incisor group of sets as well as the average result for re-

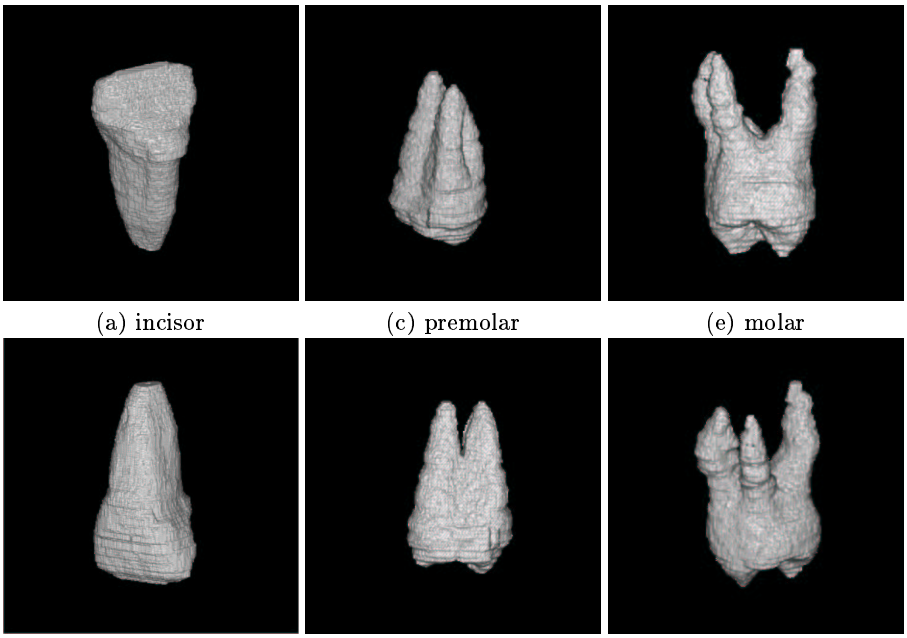

(a) incisor (c) premolar (e) molar

(b) incisor (d) premolar (f) molar

**Fig. 3.** Two different 3-D views for each of the three teeth.

constructing any intermediary slice $\hat{X}_{i+1}$ from the given group of sets $X_i$, $X_{i+2}$, for any $i \in \{1, ..., N-2\}$, where $N$ is the number of initial sets. We can observe from Table 1 that the interpolated slice obtained by morphing is closer to the original slice than that interpolated by linear interpolation. The 3-D molar reconstructed by linear interpolation is displayed in Figure 4a, while in Figure 4b we show the same molar reconstructed by morphological morphing as described in this paper.

**Table 1.** Objective comparison measure between morphological morphing and linear interpolation when reconstructing an incisor.

| Frames i,i+1,i+2 | Frame Difference (%) $\frac{\lvert XOR(X_{i+2},X_i)\rvert}{\lvert X_i\rvert}$ | Morphological Morphing (%) $\frac{\lvert XOR(\hat{X}_{i+1},X_{i+1})\rvert}{\lvert X_{i+1}\rvert}$ | Linear Interpolation (%) $\frac{\lvert XOR(\hat{X}_{i+1},X_{i+1})\rvert}{\lvert X_{i+1}\rvert}$ |
|---|---|---|---|
| 4,5,6 | 62.9 | 5.9 | 11.925 |
| 10,11,12 | 26.8 | 6.84 | 9.46 |
| 18,19,20 | 27.2 | 7.5 | 14.28 |
| Entire volume | 51.5 | 9.25 | 11.46 |

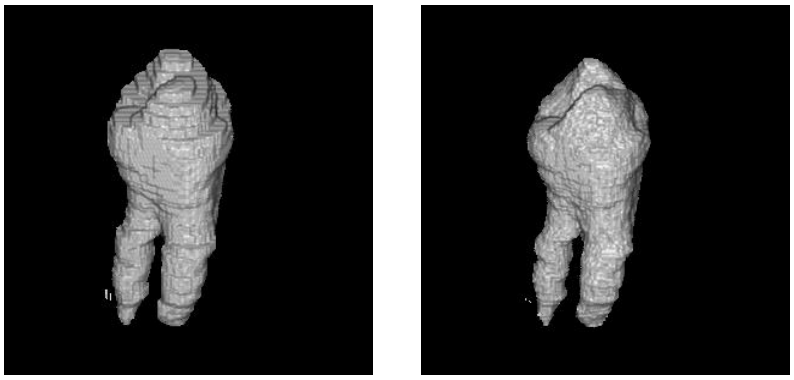

(a) Linear interpolation (b) Morphological morphing interpolation

**Fig. 4.** Reconstruction of a molar in 3-D.

After rendering and displaying the volume of a tooth, we simulate drilling by using a volumetric erosion element for the dental burr. We have chosen three different geometrical shapes for modeling the dental burr: spherical, conical and cylindrical. We associate the action of a drilling tool (dental burr) with the repetition of erosions done with various 3-D structural elements.

The 3-D structural elements employed in our experiments for simulating different types of dental burrs are shown in Figures 5a, 5b, 5c. The elementary drilling operation consists of eroding the 3-D object with the structuring element corresponding to the shape of the drilling burr. Effects of drilling on a tooth when using spherical, cylindrical and conical erosion elements are displayed in Figures 5d, 5e and 5f respectively. We have applied the proposed morphological drilling tool for virtual dentistry by testing the drilling algorithm on teeth reconstructed by 3-D interpolation. Dentists have used an entire set of virtual drilling burrs with several different geometric parameter values. A 3-D tooth after being drilled by a dentist is displayed in Figure 6a. A set of sections through the drilled tooth is shown in Figure 6b. Two dental operations that have a particular treatment significance can be observed in these figures.

## 5 Conclusions

We simulate a processing operation such as drilling on a 3-D volume given a set of sparse sets which represent parallel and equidistant object sections. We have proposed an algorithm for reconstructing the 3-D object from the given group of slices. This algorithm interpolates between each two adjacent slices by means of morphological shape-based interpolation. Virtual drilling is simulated by a succession of erosions. The proposed algorithms are applied on teeth that have been mechanically sliced and digitized. The morphological drilling algorithm can be used as a tool in a virtual sculpturing environment.

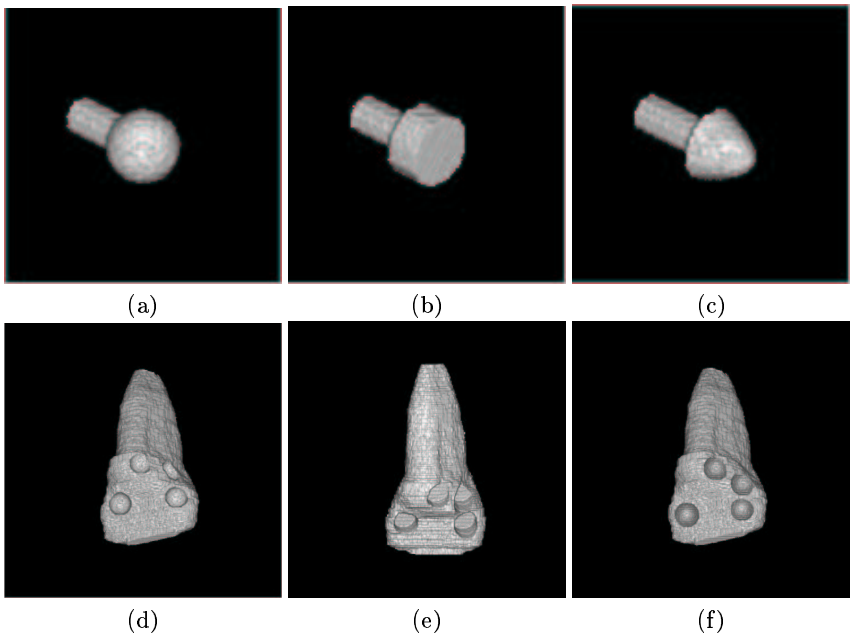


**Fig. 5.** Shapes of volumetric erosion elements employed as burrs for tooth drilling: (a) spherical; (b) cylindrical; (c) conical; (d), (e), (f) volumetric erosion results on an incisor for the given set of tools, assuming only one erosion.

## References


1. S. P. Raya, J.K. Udupa, "Shape-based interpolation of multidimensional objects," *IEEE Trans. on Medical Imaging,* vol. 9, pp. 32-42, 1990.
2. A. Goshtasby, D. A. Turner, L.V. Ackerman, "Matching of Tomographic Slices for Interpolation," *IEEE Trans. on Medical Imaging,* vol. 11, no. 4, pp. 507-516, Dec. 1992.
3. N. Nikolaidis, I. Pitas, *3-D Image Processing Algorithms.* J. Wiley & Sons, 2000.
4. M. Moshfeghi, "Directional Interpolation for Magnetic Resonance Angiography Data," *IEEE Trans. on Medical Imaging,* vol. 12, no. 2, pp. 366-379, June 1993.
5. W. E. Higgins, C. J. Prlick, B. E. Ledell, "Nonlinear Filtering Approach to 3-D Grey-Scale Image Interpolation," *IEEE Trans. on Medical Imaging*, vol. 15, no. 4, pp. 580-587, 1996.
6. J. D. Boissonnat, "Shape reconstruction from planar cross-sections," *Computer Vision, Graphics and Image Processing,* vol. 44, no. 1, pp. 1-29, 1988.
7. P.N. Werahera, G.J. Miller. G.D. Taylor, T. Brubaker, F. Daneshgari, E.D. Crawford, "A 3-D Reconstruction Algorithm for Interpolation and Extrapolation of Planar Cross Sectional Data," *IEEE Trans. on Medical Imaging,* vol 14, no. 4, pp. 765-771, Dec 1995.

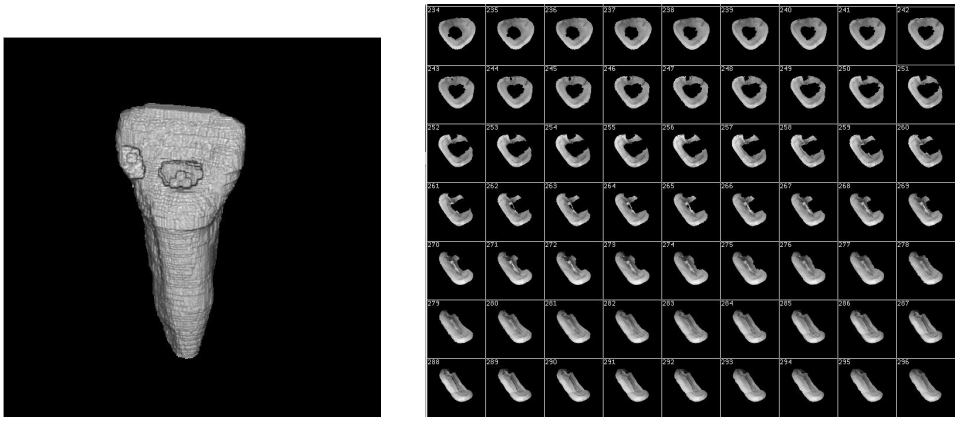

(a) (b)

**Fig. 6.** Incisor treatment simulation: (a) 3-D view of the drilled incisor; (b) drilling effects on cross-sectional slices through incisor.


8. W.E. Higgins, C. Morice, E. L. Ritman, "Shape-based interpolation of tree-like structures in three-dimensional images," *IEEE Trans. on Medical Imaging,* vol. 12, no. 3, pp. 439-450, Sep. 1993.
9. S.-Y. Chen, W.-C.. Lin, C.-C. Liang, C.-T. Chen, "Improvement on Dynamic Elastic Interpolation Technique for Reconstructing 3-D Objects from Serial Cross Sections," *IEEE Trans. on Medical Imaging,* vol. 9, no. 1, pp. 71-83, March 1990.
10. M. Joliot, B. M. Mazoyer, "Three-Dimensional Segmentation and Interpolation of Magnetic Resonance Brain Images," *IEEE Trans. on Medical Imaging,* vol. 12, no. 2, pp. 269-277, June 1993.
11. G. J. Grevera, J.K. Udupa, "Shape-Based Interpolation of Multidimensional Grey-level images," *IEEE Trans. on Medical Imaging*, vol. 15, no. 6, pp. 881-892, 1996.
12. S. Beucher, "Sets, partitions and functions interpolations," *International Symposium on Mathematical Morphology and its Applications to Image and Signal Processing IV*, Amsterdam, Netherlands, June 3-5, 1998, pp. 307-314.
13. J. Sera, *Image Analysis and Mathematical Morphology.* New York: Academic Press, 1982.
14. R. Yoshida, T. Miyazawa, A. Doi, T. Otsuki, "Clinical Planning Support System - CliPSS," *IEEE Computer Graphics and Applications*, vol 13, no. 6, pp. 76-84, Nov. 1993.